MINI-RF OBSERVATIONS OF RADAR SCATTERING BEHAVIOR OF YOUNG LUNAR CRATERS AND IMPLICATIONS FOR RELATIVE CRATER AGE DATING. A. M. Stickle[1], G. W. Patterson[1], M. Slade[2], M. C. Nolan[3], P. Taylor[4], G. A. Morgan[5], G. D. Tolometti[6], and the Mini-RF team [1]Johns Hopkins Applied Physics Laboratory, 11100 Johns Hopkins Rd., Laurel, MD, USA 20723, angela.stickle@jhuapl.edu; [2]Jet Propulsion Laboratory, Pasadena CA; [3]University of Arizona, Phoenix, AZ; [4]NRAO, Greenbank, WV; [5]Planetary Science Institute, Washington DC; [6]Western University, London, Ontario.

Introduction: During the last two extended science missions, the Mini-RF instrument onboard NASA's Lunar Reconnaissance Orbiter (LRO) has acquired bistatic radar data of the lunar surface at both S-band (12.6 cm) and X-band (4.2 cm) wavelengths in an effort to understand the scattering properties of lunar terrains as a function of bistatic angle (e.g., **Figure 1**). At optical wavelengths, previous studies demonstrated that the material properties of lunar regolith can be sensitive to variations in phase angle [1-3]. This sensitivity gives rise to the lunar opposition effect and likely involves contributions from shadow hiding at low phase angles and coherent backscatter near zero phase [1]. Mini-RF bistatic data of lunar materials indicate that such behavior can also be observed at the wavelength scale of X- and S-band radar. These observations represent the first time spatially resolved information on this effect to have been measured for the Moon at radar wavelengths. The ejecta blankets of ten lunar craters have been observed to date (three of the craters at both X- and S-band), and their Circular Polarization Ratios (CPRs) have been characterized as a function of phase (bistatic) angle. Work to characterize other radar products (e.g., total backscattered power, polarization products) is ongoing. Observing the scattering behavior of continuous ejecta blankets at multiple radar wavelengths can provide information regarding the size/frequency of scatterers emplaced as ejecta, as well as unique insight into the rate of regolith formation on the Moon.

Bistatic Operations: Radar observations of planetary surfaces provide important information on the structure (i.e., roughness) and dielectric properties of surface and buried materials [4-7]. These data can be acquired using a monostatic architecture, where a single antenna serves as the signal transmitter and receiver, or they can be acquired using a bistatic architecture, where a signal is transmitted from one location and received at another. The former provides information on the scattering properties of a target surface at zero bistatic angle. The latter provides this same information but over a variety of bistatic (phase) angles. The bistatic (phase) angle is a function of the angle between the incident radiation to the surface and the backscattered radiation.

The Mini-RF instrument is currently operating in a bistatic architecture with the Goldstone DSS-13 antenna in California. Prior to its collapse in 2020, the Arecibo Observatory (AO) in Puerto Rico had served as the transmitter for S-band operations, while DSS-13 serves as the transmitter for X-band operations. Mini-RF serves as the receiver in both cases. This architecture maintains the hybrid dual-polarimetric nature of the Mini-RF instrument [8] and, therefore, allows for the calculation of the Stokes parameters (S_1, S_2, S_3, S_4) that characterize the backscattered signal (and the products derived from those parameters).

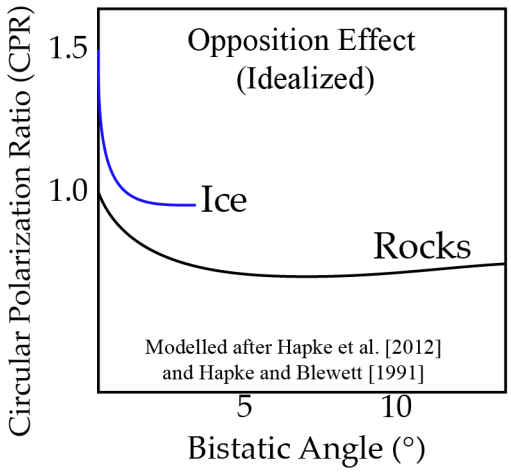

Figure 1. Idealized behavior of CPR as a function of bistatic angle for wavelength-scale ice and rocks, showing opposition effect [1]. Mini-RF is currently observing lunar terrains to measure this function directly.

S-band observations: A product derived from the Stokes parameters (S) is the CPR, or $\mu_c = (S_1-S_4)/(S_1+S_4)$. CPR information is commonly used in analyses of planetary radar data [4-7], and is a representation of surface roughness at the wavelength scale of the radar (i.e., surfaces that are smoother at the wavelength scale will have lower CPR values and surfaces that are rougher will have higher CPR values). High CPR values (> 1) can also serve as an indicator of the presence of water ice [9].

Earlier studies, at S-band [e.g., 10], showed that the ejecta of some young lunar craters exhibited behavior similar to a coherent backscatter opposition effect (CBOE) when examined in radar data. The style of the observed CBOE differs between craters, which may indicate differences in ejecta fragment formation or emplacement.

Four of the craters examined in S-band (*Byrgius A*, *Aristarchus*, *La Condamine S*, and *Kepler*) exhibit CPR characteristics suggestive of an opposition effect: higher CPR at lower bistatic (phase) angle. The increase in CPR occurs near 2–4 degrees bistatic angle. These craters occur in both highlands and mare regions, and are all characterized as young. Three other examined craters (*Bouguer*, *Harpalus*, *Anaxagoras*) exhibit CPR that remains relatively constant across bistatic angle. This may be for a couple reasons: (1) The craters are older (though most are still Copernican), and thus likely smoother, so that the opposition effect will be less pronounced; or (2) insufficient data have been acquired to characrerize the opposition behavior of the crater ejecta. That is to say, an opposition effect may be present, but the craters have not yet been observed under the conditions needed to detect it. *Schomberger A*, *La Condamine S*, and *Kepler* exhibit scattering properties as a function of bistatic angles that differ from the other observed craters, with areas of relatively constant CPR across bistatic angles. The oldest crater observed (*Hercules*, which is classified as Eratosthenian) shows no indication of an opposition response across phase angle space.

Patterson *et al*. [11] suggest that the radar scattering characteristics of the continuous ejecta for craters, coupled with age estimates based on crater statistics and geologic mapping, imply a relationship between the opposition response of the ejecta and the age of the crater. Thus, recording the CPR response as a function of bistatic angle may be a way to determine relative age between deposits.

X-band Observations: The Mini-RF X-band bistatic data are currently being reprocessed with updated calibration parameters, which significantly increases the quality of the derived data products (e.g., CPR).

X-band observations of *Anaxagoras* and *Kepler* (**Figure 2**) also suggest an opposition surge at low bistatic angle in X-band, though the observed response is weaker at *Kepler* crater than at *Anaxagoras*. Both *Kepler* and *Anaxagoras* were observed at S-band as well, and showed signatures indicative of an opposition response. Observing the scattering behavior in multiple wavelengths may provide further information about the rate of breakdown of rocks of varying size to provide increased understanding of how impacts produce regolith on the Moon, especially when differences are seen, as in this case. To preserve an opposition effect at S-band and not X-band, observations suggest the scattering signature at *Kepler* crater is dominated by larger-scale scatterers (e.g., boulders) on the order of meters to 10s of meters. *Anaxagoras*, on the other hand, has both large and smaller scatterers; thus an opposition effect is seen in both radar wavelengths. *Anaxagoras* is estimated to be 300 Ma [12] in age, compared to *Kepler* at 625–1250 Ma [13-15], which may explain why smaller scatterers are still present at *Anaxagoras* but have begun to break down at *Kepler*.

References: [1] Hapke et al. (1998), *Icarus*, 133, 89-97; [2] Nelson et al. (2000), *Icarus*, 147, 545-558; [3] Piatek et al. (2004), *Icarus*, 171, 531-545. [4] Campbell et al. (2010), *Icarus*, 208, 565-573; [5] Raney et al. (2012), *JGR,* 117, E00H21; [6] Carter et al. (2012), *JGR,* 117, E00H09; [7] Campbell (2012), *JGR*, 117, E06008; [8] Raney, R. K. et al. (2011), *Proc. of the IEEE*, 99, 808-823; [9] Black et al. (2001), *Icarus*, 151, 167-180; [10] Stickle et al. (2018) *LPSC* Abstract #2007; [11] Patterson, et al. (2017), *Icarus*, 283, 2-19; [12] M. Kirchoff, personal communicaton; [13] Koenig et al. (1977) *Proc. LPSC*, 8, p. 555; [14] Baldwin (1985) *Icarus* 61, 63-91; [15] Ulrich (1969) USGS Map I-604(LAC-11);.

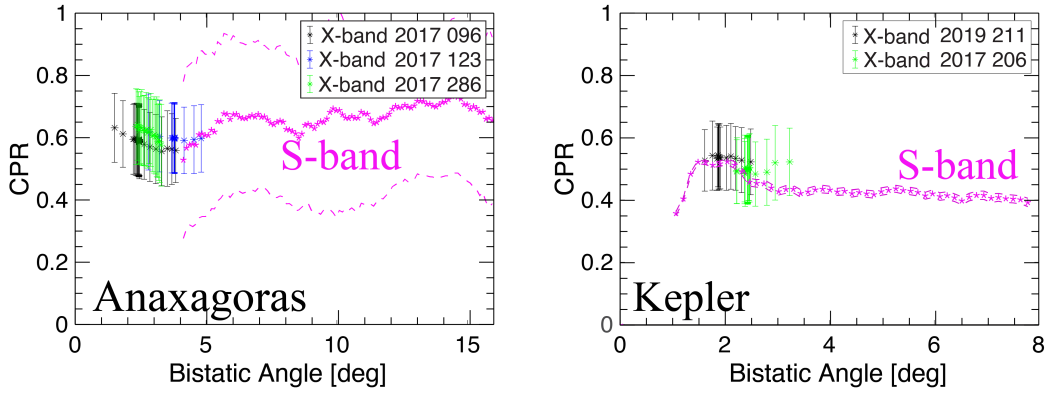

Figure 2. CPR as a function of bistatic angle for Anaxagoras (left) and Kepler Crater (right). The curves are made up of data from several individual X-band collects over ESM3 and ESM4 and S-band collects (magenta) from ESM1 and ESM3. At X-band, Anaxagoras ejecta shows a clear opposition effect behavior, while Kepler crater is a more muted response. The error bars represent one standard deviation in the data.